

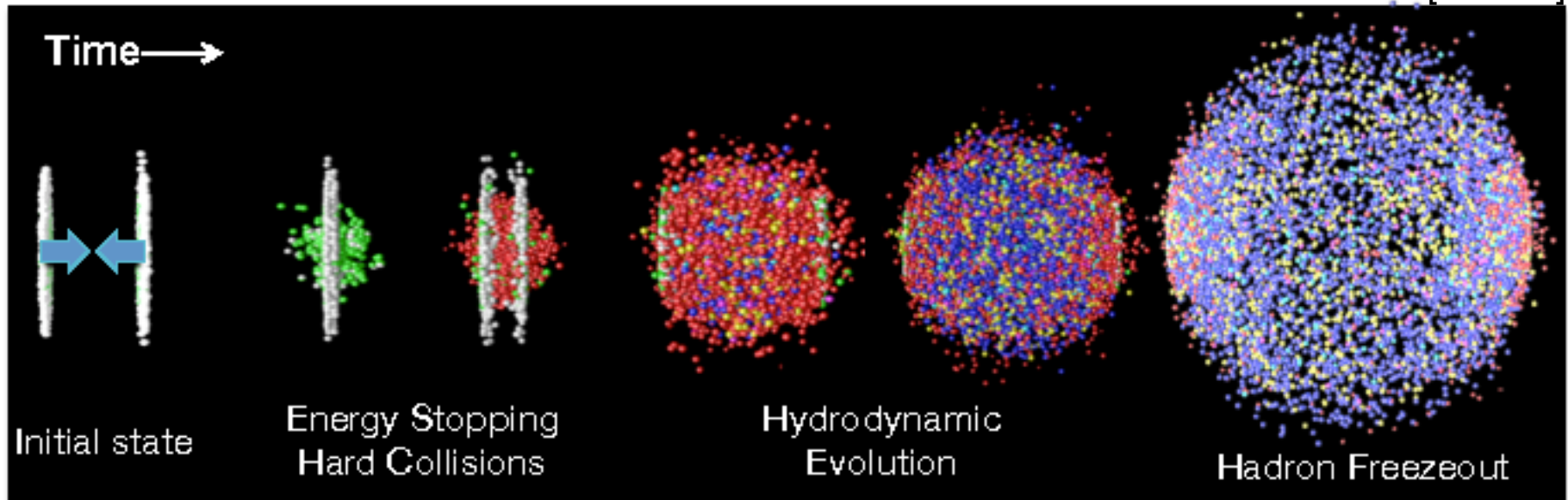
Azimuthal angle dependence of HBT radii with respect to the Event Plane in Au+Au collisions at PHENIX

Takafumi Niida for the PHENIX Collaboration
University of Tsukuba

WWND2014 @Galveston, USA

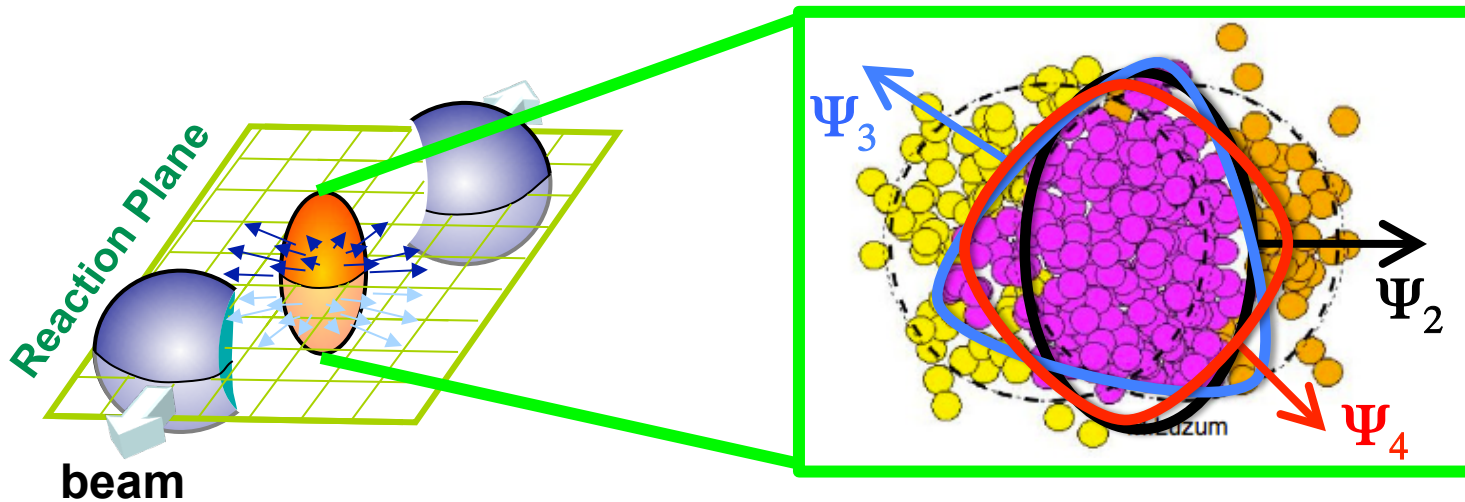
Space-Time evolution in HI collisions

arXiv:1201.4264 [nucl-ex]



- Final emitting particles carry information on the properties of the QGP and its space-time evolution
- Space-time picture of the system evolution is emerging from recent studies at RHIC and the LHC

Momentum anisotropy at final state



- Initial source eccentricity with fluctuations leads to momentum anisotropy at final state, known as higher harmonic flow v_n

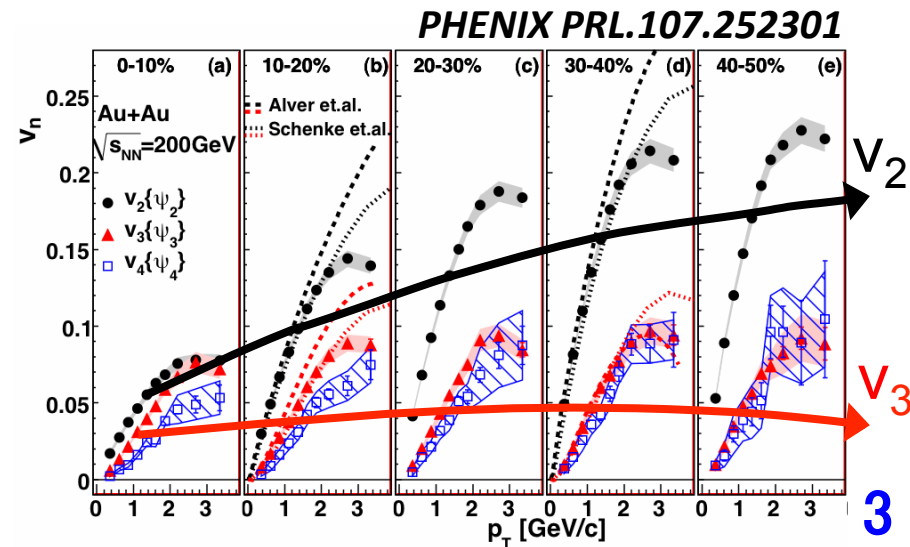
✧ Sensitive to η/s (PRL107.252301)

$$\frac{dN}{d\phi} \propto 1 + 2 \sum v_n \cos[n(\phi - \Psi_n)]$$

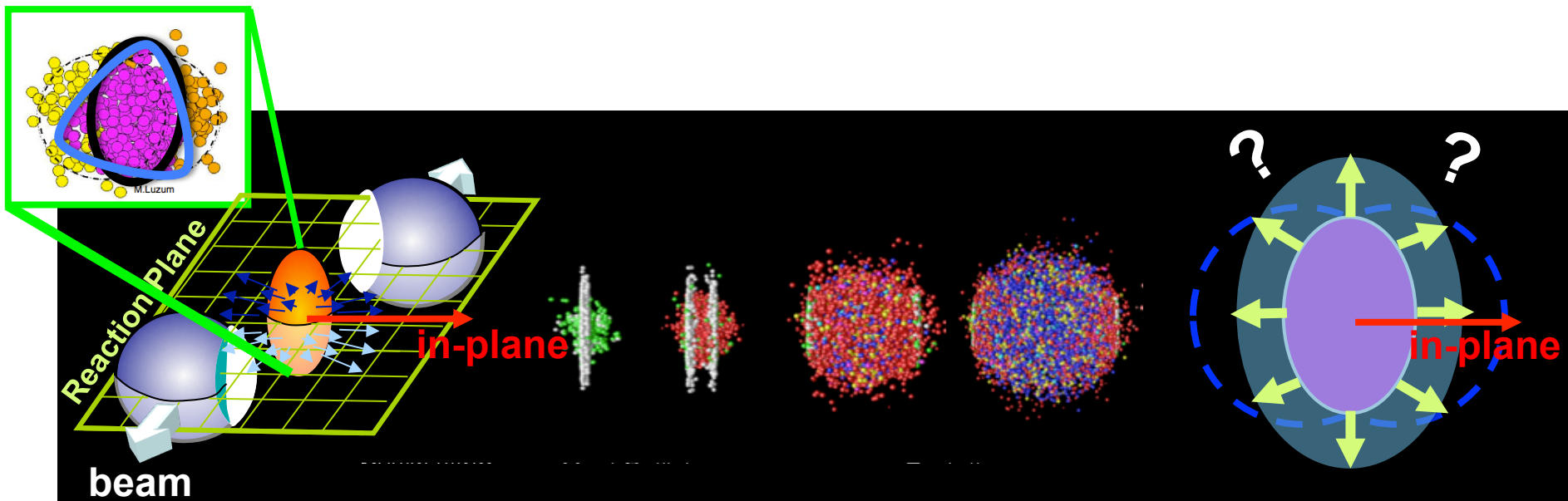
$$v_n = \langle \cos[n(\phi - \Psi_n)] \rangle$$

Ψ_n : higher harmonic event plane

ϕ : azimuthal angle of emitted particles



Spatial anisotropy at final state



■ What is the final source shape?

- ✧ Spatial-extent at final state depends on the magnitude of initial eccentricity with fluctuation, the strength of flow, expansion time, and viscosity
- ✧ Does the initial fluctuation also remain at final state?

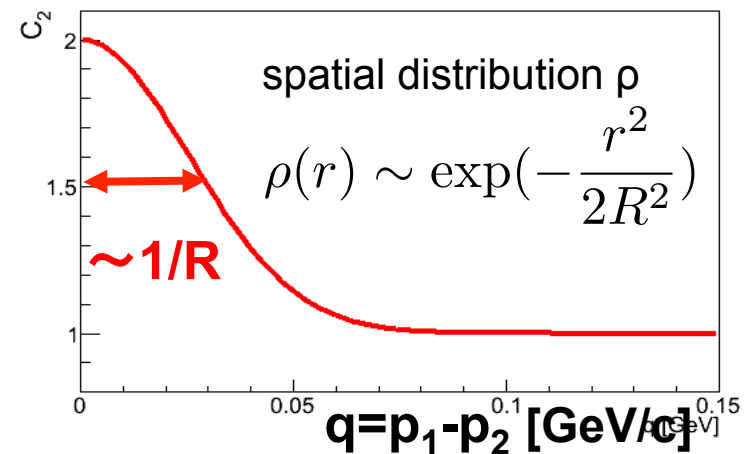
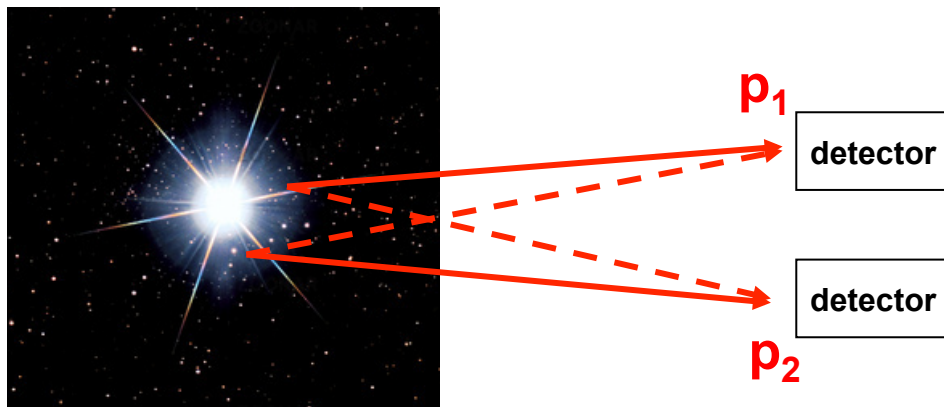
■ HBT interferometry relative to different event plane could probe them.

HBT Interferometry

- 1956, **H. Brown** and **R. Twiss**, measured angular diameter of Sirius
- 1960, Goldhaber *et al.*, correlation among identical pions in $p+\bar{p}$
- By quantum interference between two identical particles

wave function for 2 bosons(fermions) : $\Psi_{12} = \frac{1}{\sqrt{2}} [\Psi(x_1, p_1)\Psi(x_2, p_2) \pm \Psi(x_2, p_1)\Psi(x_1, p_2)]$

$$C_2 = \frac{P(p_1, p_2)}{P(p_1)P(p_2)} \approx 1 + |\tilde{\rho}(q)|^2 = 1 + \exp(-R^2 q^2)$$

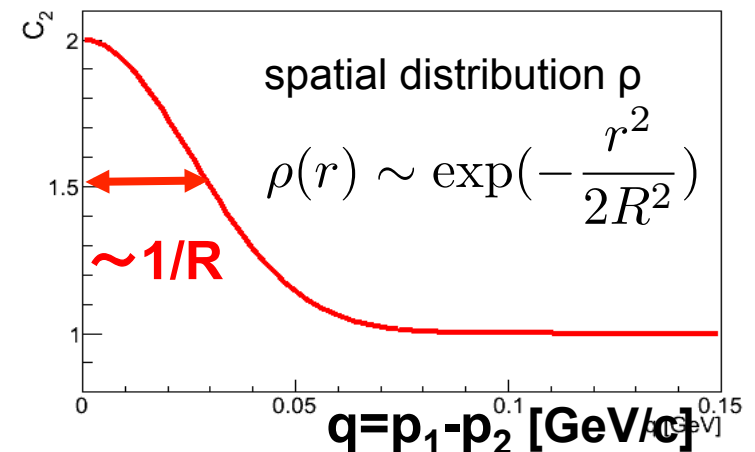
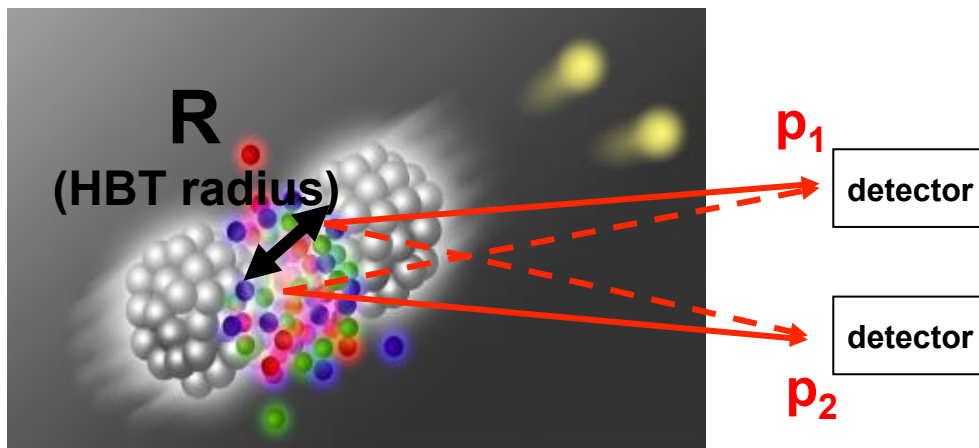


HBT Interferometry

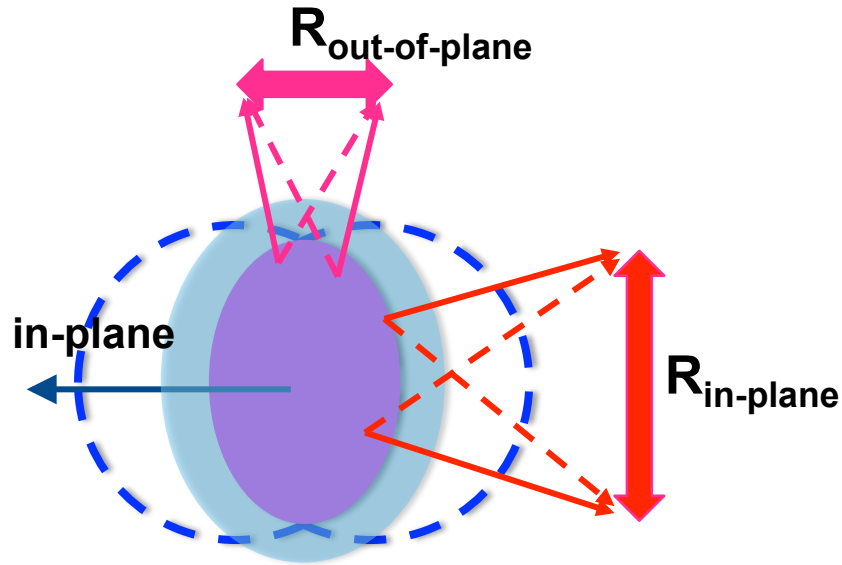
- 1956, **H. Brown** and **R. Twiss**, measured angular diameter of Sirius
- 1960, Goldhaber *et al.*, correlation among identical pions in $p+\bar{p}$
- By quantum interference between two identical particles

wave function for 2 bosons(fermions) : $\Psi_{12} = \frac{1}{\sqrt{2}} [\Psi(x_1, p_1) \Psi(x_2, p_2) \pm \Psi(x_2, p_1) \Psi(x_1, p_2)]$

$$C_2 = \frac{P(p_1, p_2)}{P(p_1)P(p_2)} \approx 1 + |\tilde{\rho}(q)|^2 = 1 + \exp(-R^2 q^2)$$



Azimuthal sensitive HBT w.r.t 2nd-order event plane

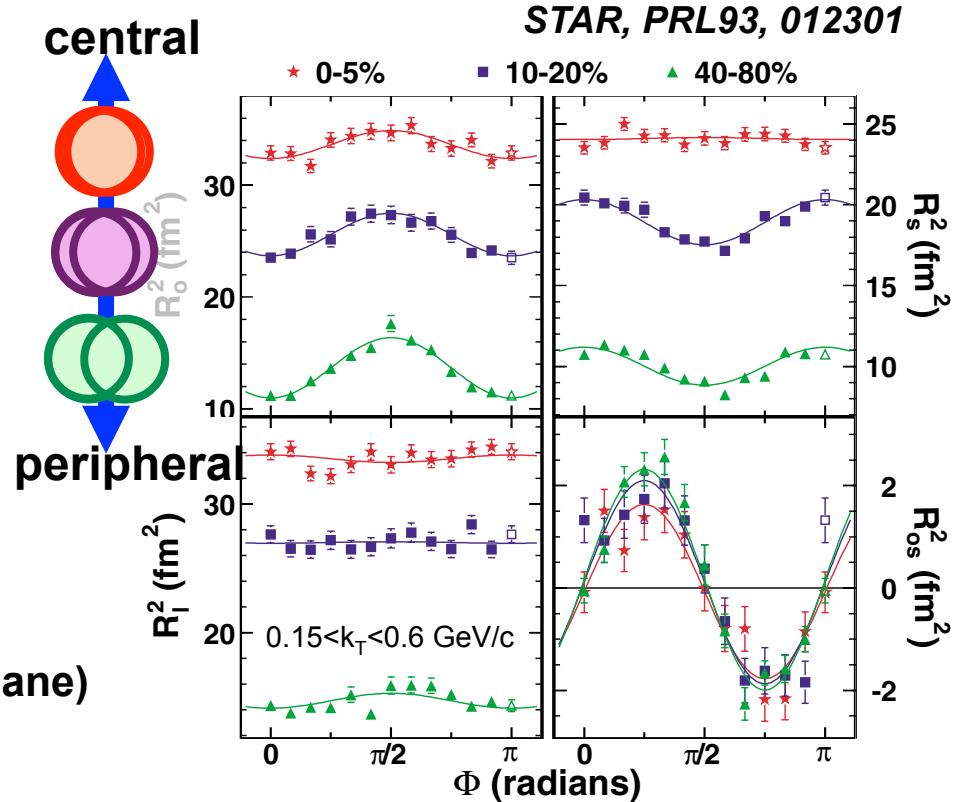


Reaction plane \approx 2nd-order event plane (v_2 plane)

PRC70, 044907 (2004), Blast-wave model

$$R_{s,n}^2 = \left\langle R_{s,n}^2(\Delta\phi) \cos(n\Delta\phi) \right\rangle$$

$$\varepsilon_{final} = 2 \frac{R_{s,2}^2}{R_{s,0}^2}$$

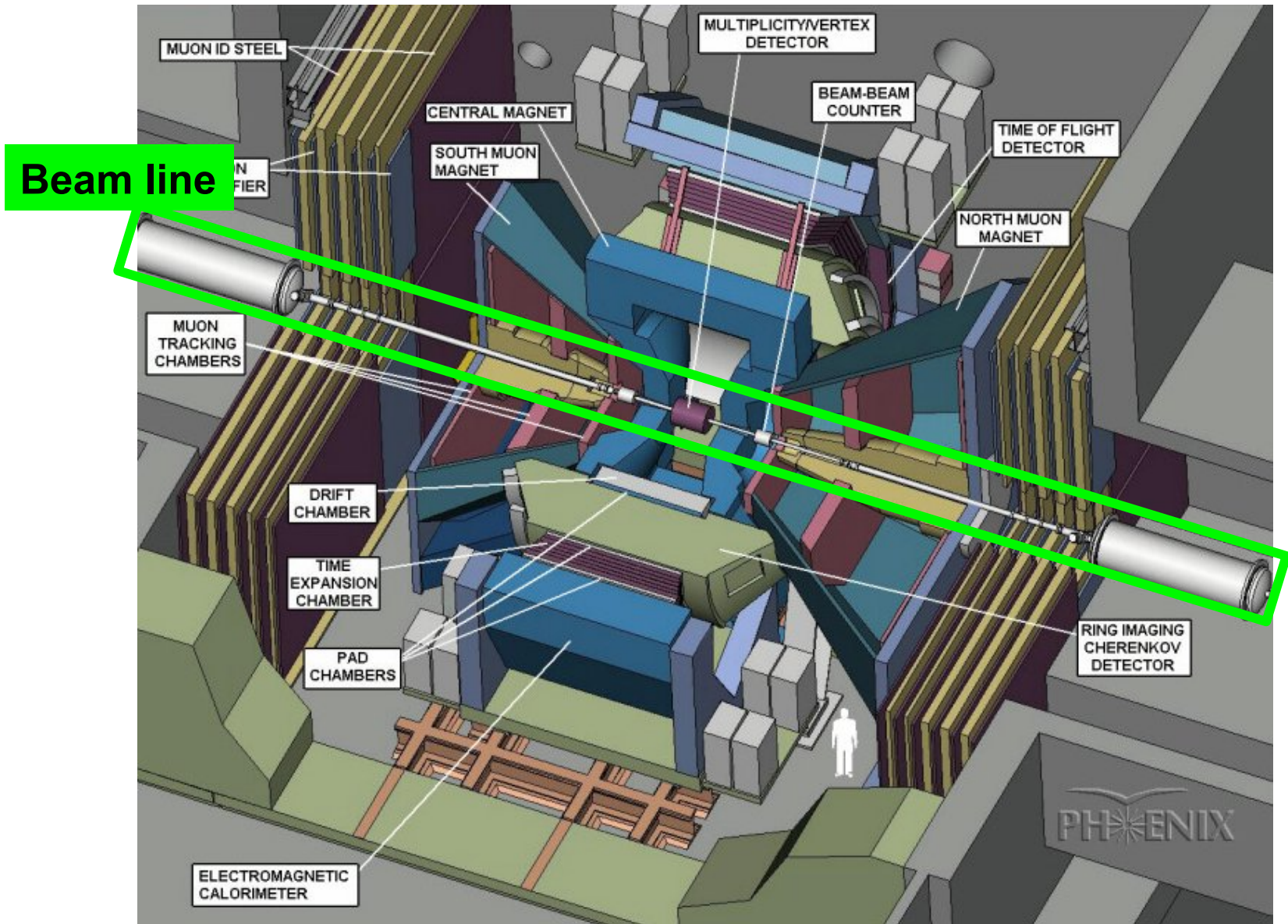


■ $R_{s,2}$ is sensitive to final eccentricity

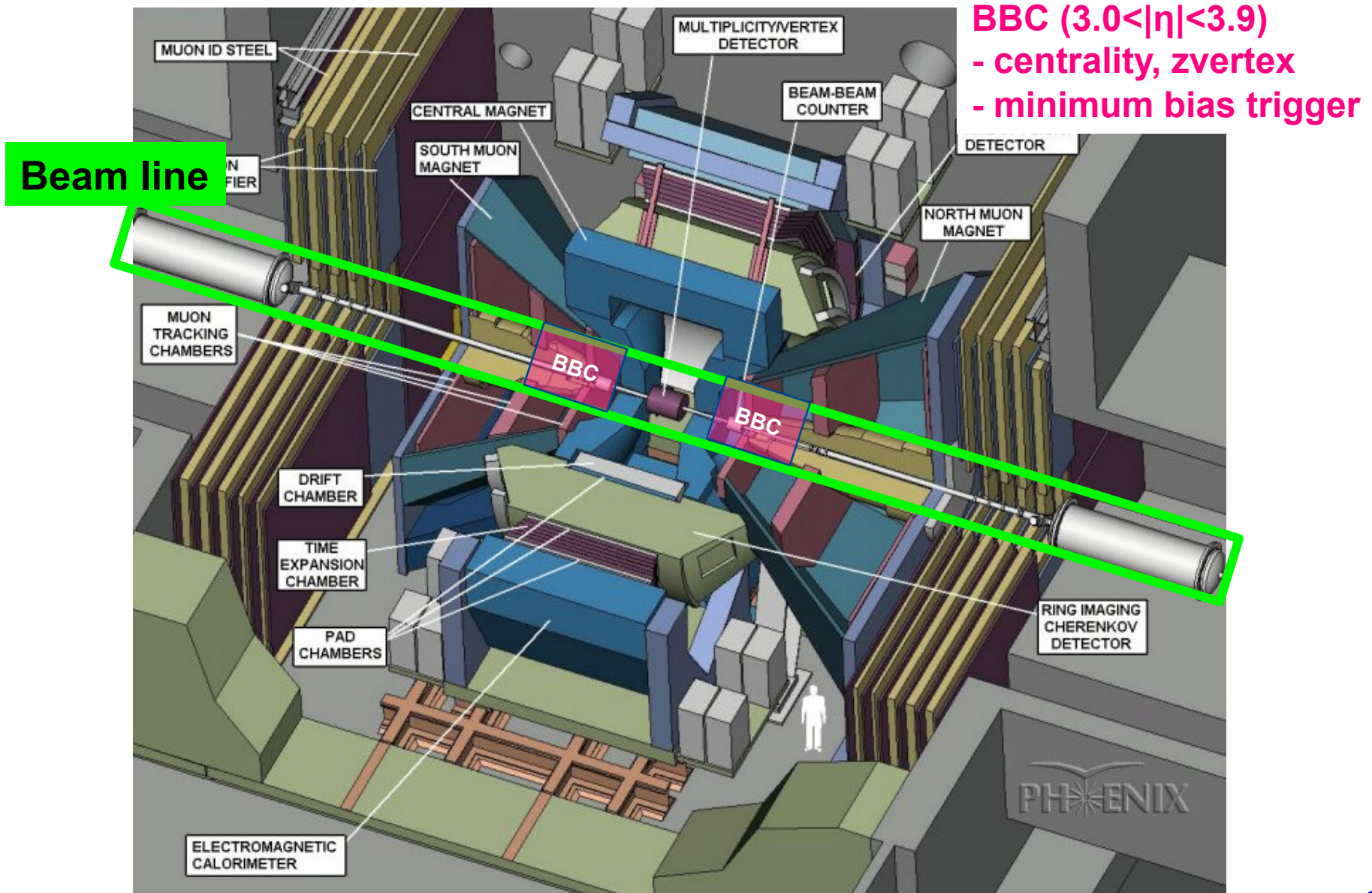
✧ Oscillation indicates elliptical shape extended to out-of-plane direction.

Results of HBT w.r.t 2nd- and 3rd-order event planes are presented today!

PHENIX Experiment

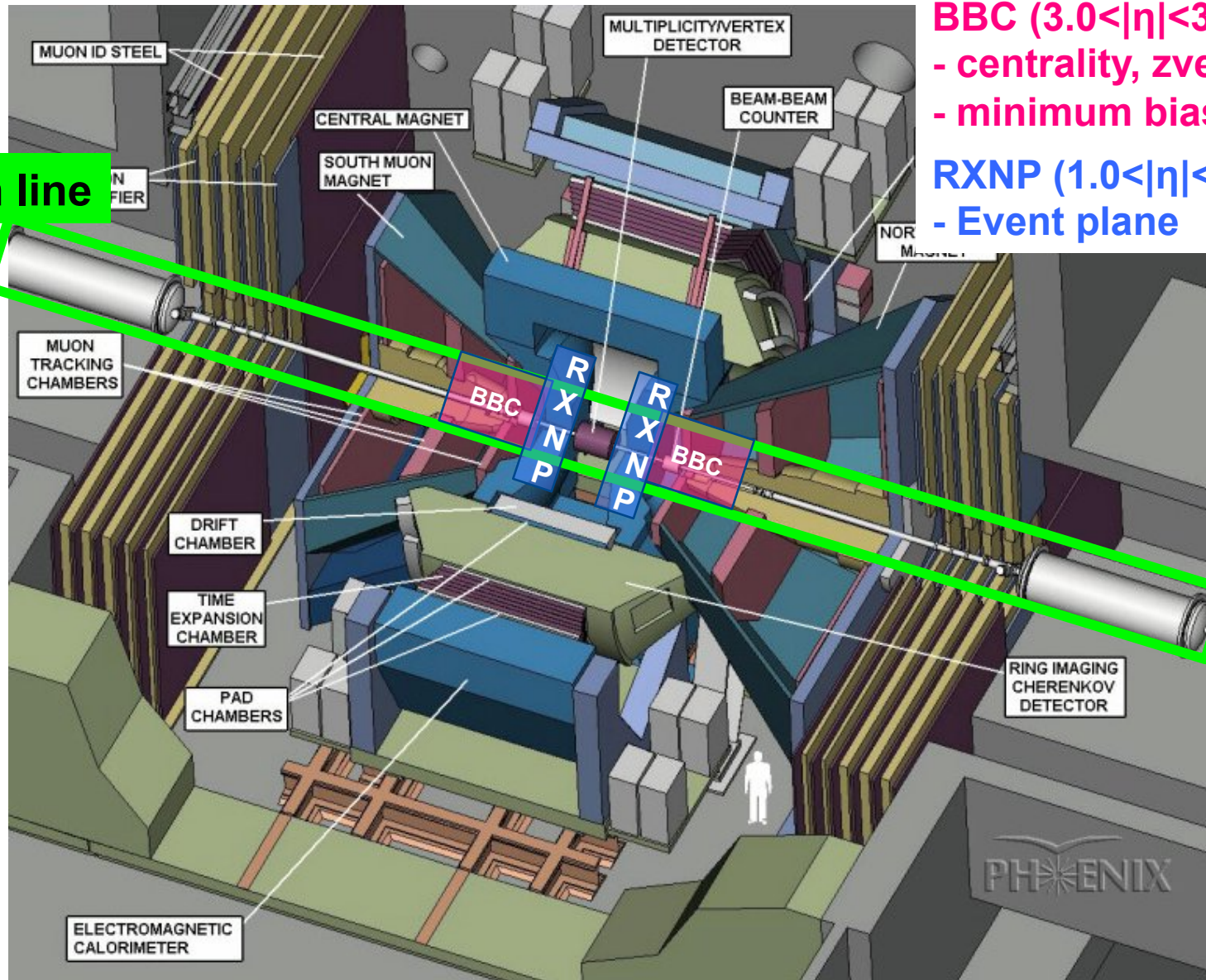


PHENIX Experiment



PHENIX Experiment

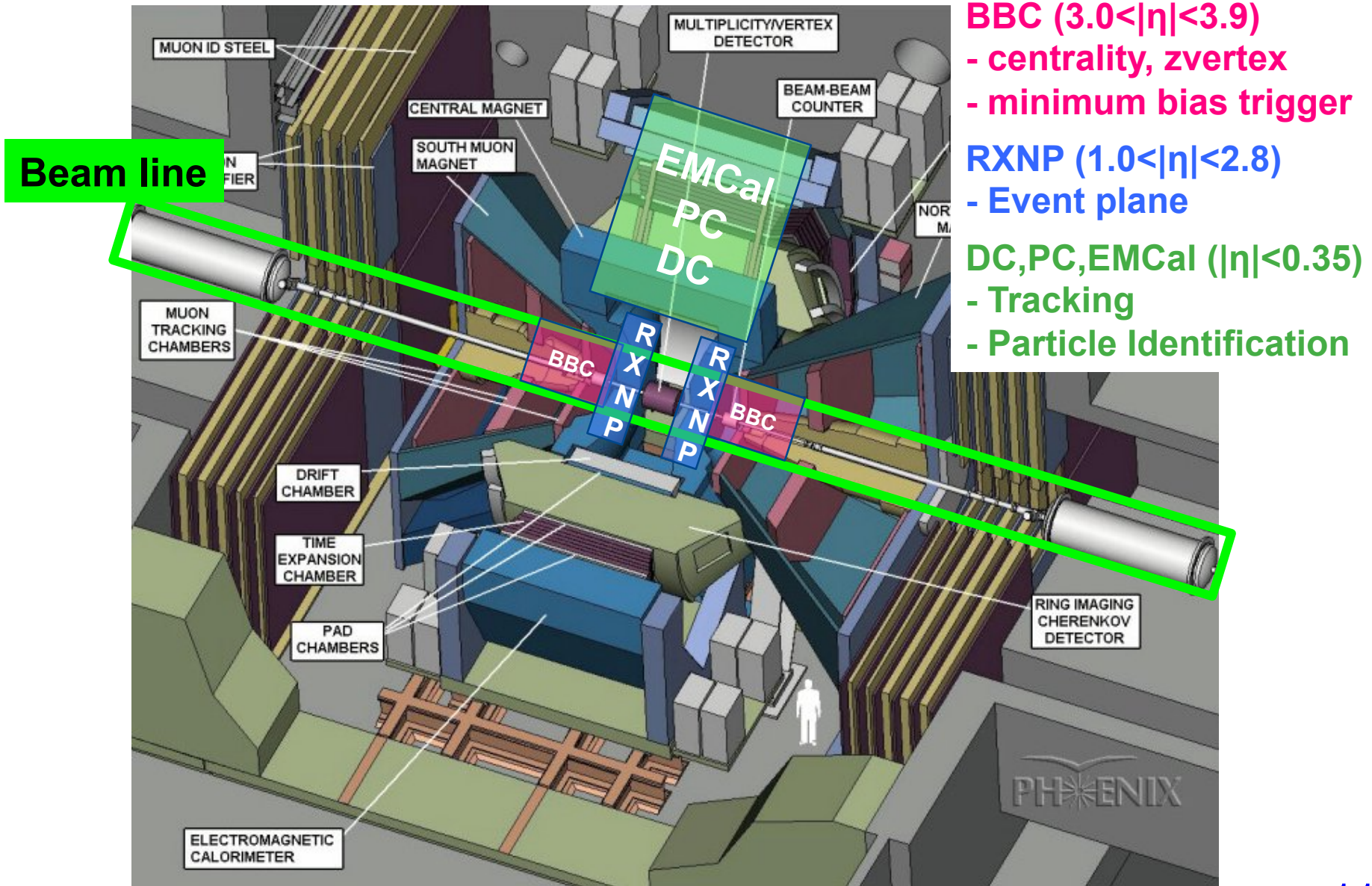
Beam line



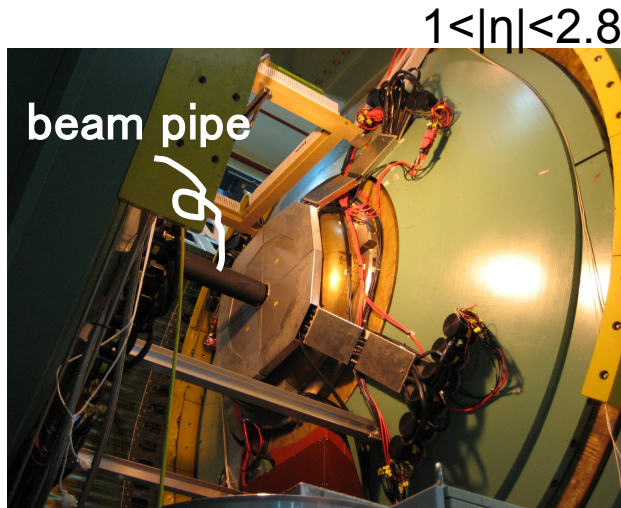
BBC ($3.0 < |\eta| < 3.9$)
- centrality, zvertex
- minimum bias trigger

RXNP ($1.0 < |\eta| < 2.8$)
- Event plane

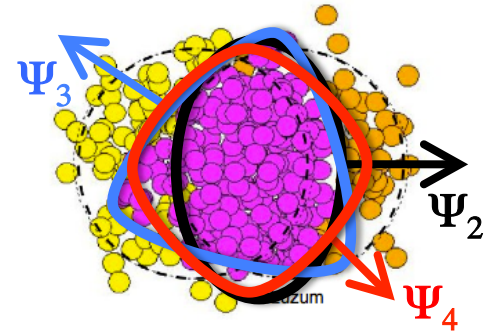
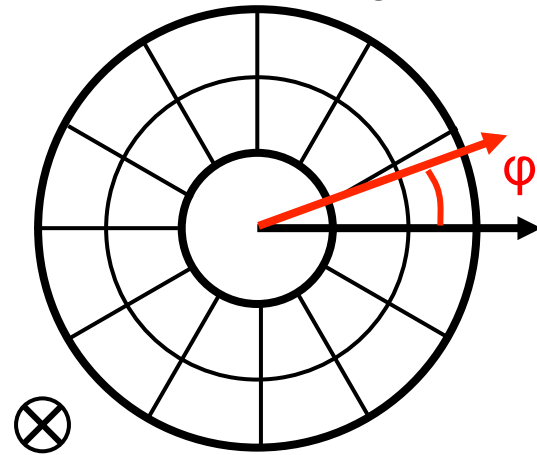
PHENIX Experiment



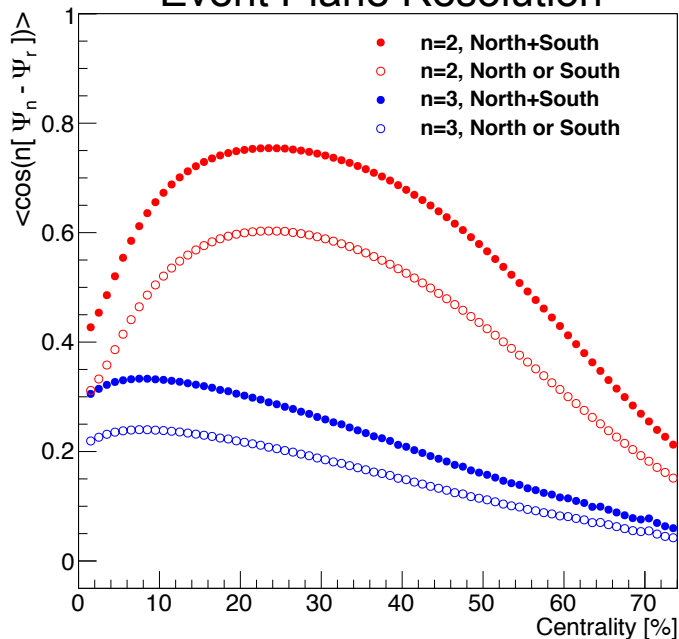
Event Plane Determination



24 scintillator segments



Event Plane Resolution



- Determined by anisotropic flow itself using Reaction Plane Detector

$$\Psi_n = \frac{1}{n} \tan^{-1} \left(\frac{\sum w_i \cos(n\phi_i)}{\sum w_i \sin(n\phi_i)} \right)$$

- EP resolutions $\langle \cos[n(\Psi_n - \Psi_{real})] \rangle$

✧ $\text{Res}\{\Psi_2\} \sim 0.75$, $\text{Res}\{\Psi_3\} \sim 0.34$

Particle Identification

- **EMC-PbSc is used.**

- ✧ timing resolution ~ 600 ps

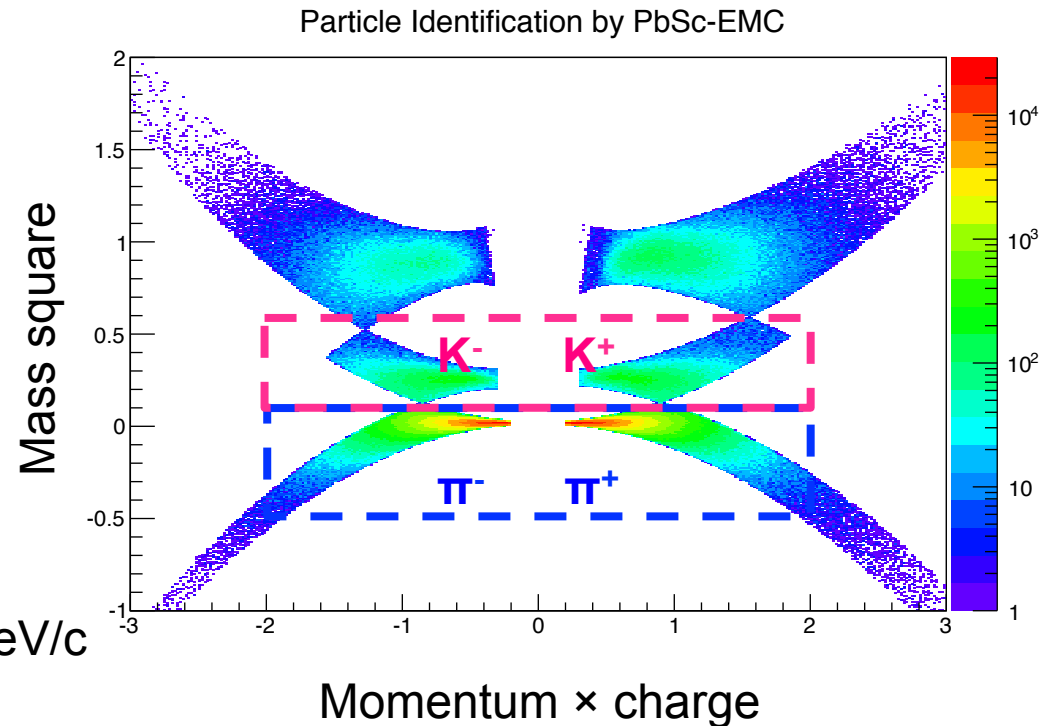
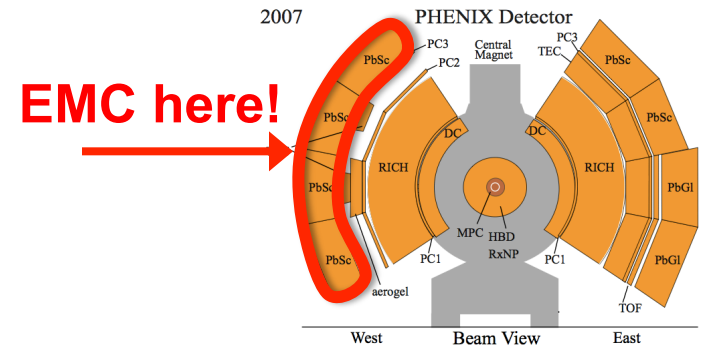
- **Time-Of-Flight method**

$$m^2 = p^2 \left(\left(\frac{ct}{L} \right)^2 - 1 \right)$$

p: momentum L: flight path length
t: time of flight

- **Charged π within 2σ**

- ✧ π/K separation up to ~1 GeV/c



3D-HBT Analysis

■ Core-Halo picture with “Out-Side-Long” frame

- ✧ Longitudinal center of mass system ($p_{z1}=p_{z2}$)
- ✧ taking into account long lived decay particles

$$C_2 = C_2^{core} + C_2^{halo}$$

$$= [\lambda(1 + G)F_{coul}] + [1 - \lambda]$$

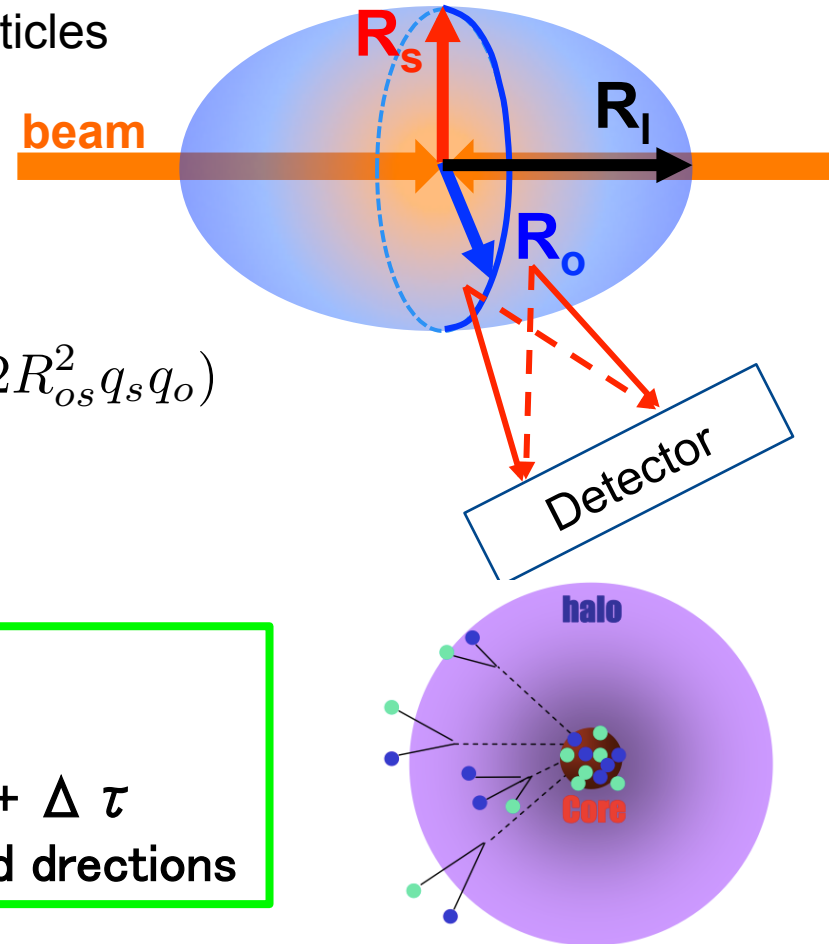
$$G = \exp(-R_s^2 q_s^2 - R_o^2 q_o^2 - R_l^2 q_l^2 - 2R_{os}^2 q_s q_o)$$

F_{coul} : Coulomb correction factor
 λ : fraction of pairs in the core

R_l = Longitudinal Gaussian source size
 R_s = Transverse Gaussian source size
 R_o = Transverse Gaussian source size + $\Delta \tau$
 R_{os} = Cross term b/w side- and outward directions

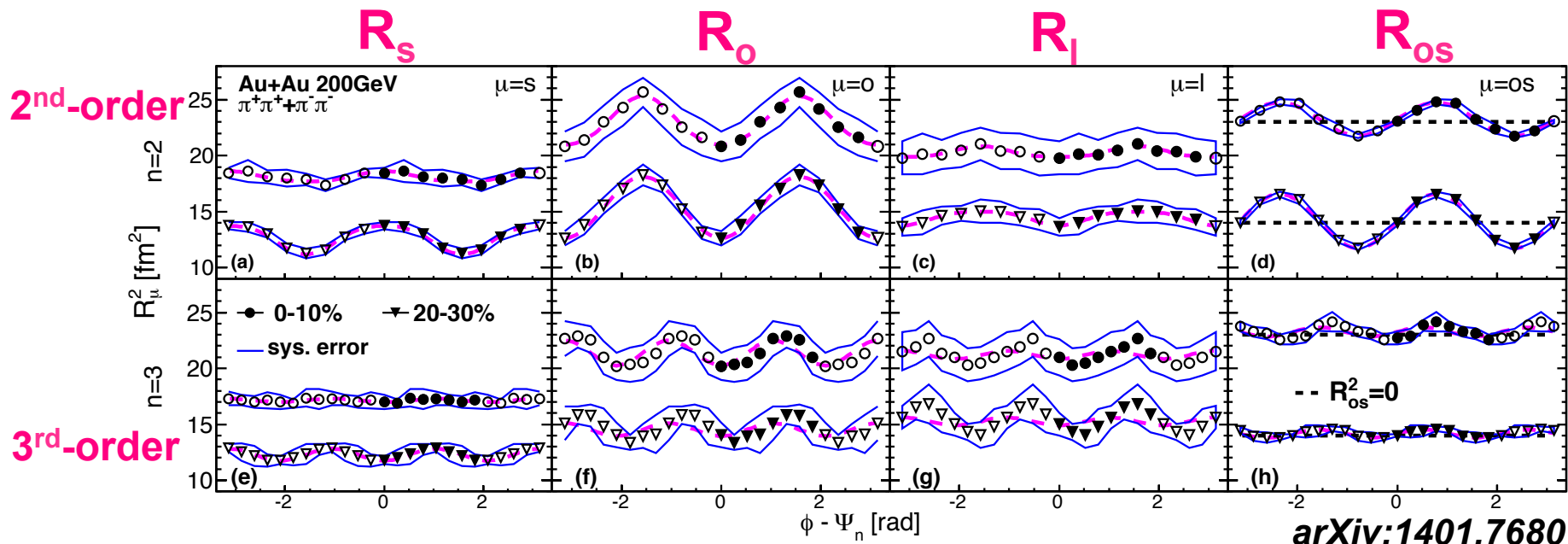
$$\vec{k}_T = \frac{1}{2}(\vec{p}_{T1} + \vec{p}_{T2})$$

$$\vec{q}_o \parallel \vec{k}_T, \quad \vec{q}_s \perp \vec{k}_T$$



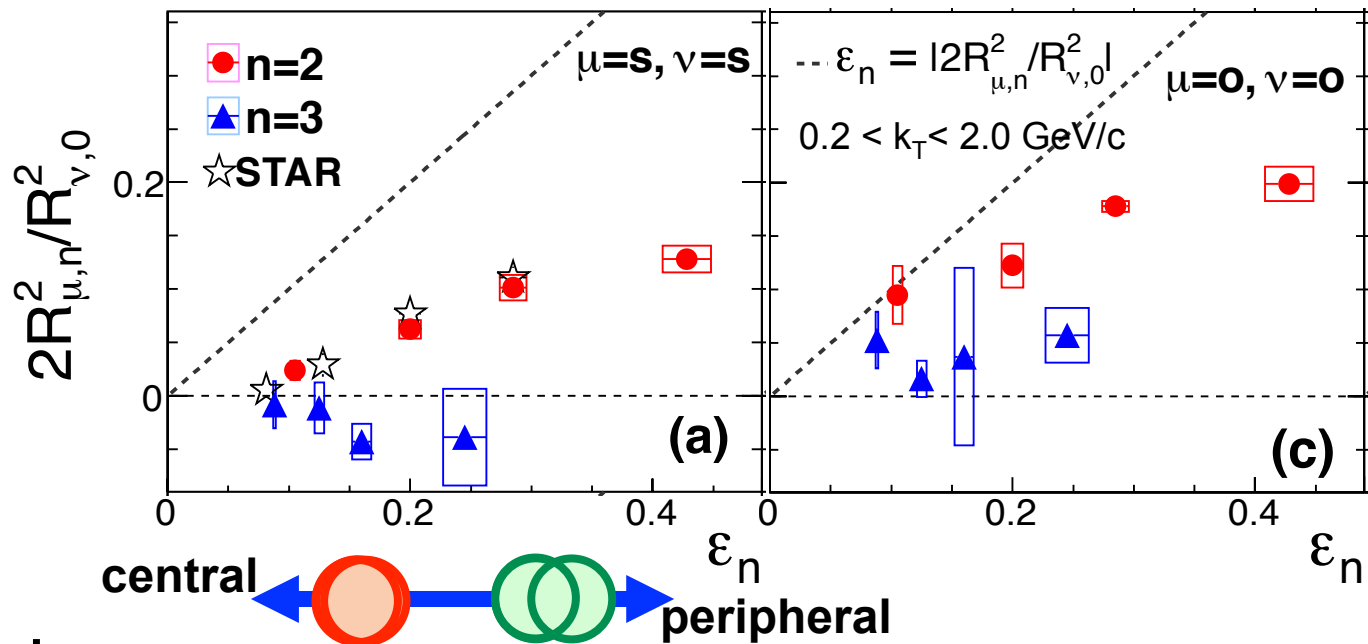
RESULTS

HBT radii w.r.t 2nd- and 3rd-order event planes



- Oscillation w.r.t Ψ_2 could be intuitively explained by out-of-plane extended elliptical source
 - ✧ Opposite sign of R_s and R_o
- For Ψ_3 , weak but finite oscillations can be seen, especially in R_o
 - ✧ Same sign of R_s and R_o in 20-30% centrality
- R_o oscillation $>$ R_s oscillation for both orders

Initial ε_n vs oscillation amplitudes



■ 2nd-order

- ✧ $2R_{s,2}^2/R_{s,0}^2 \sim$ final source eccentricity under the BW model, and consistent with STAR result
- ✧ $\varepsilon_{\text{final}} \approx \varepsilon_{\text{initial}}/2$, source eccentricity is reduced, but still retain initial shape extended out-of-plane

■ 3rd-order

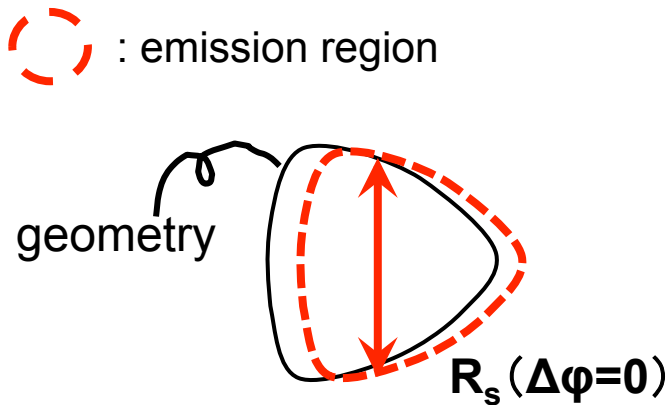
- ✧ Weaker oscillation and no significant centrality(ε_n) dependence
- ✧ $R_{s,3}^2 \leq 0$ and $R_{o,3}^2 \geq 0$ are seen in all centralities.

■ Does this result indicate non spatial triangularity at final state?

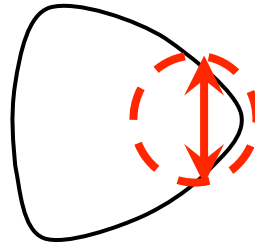
Triangular deformation can be observed via HBT?

- HBT radii w.r.t Ψ_3 don't almost show oscillation in a static source, but it appears in a expanding source. (S. Voloshin, J. Phys. G38, 124097)
- Initial triangularity is weaker than initial eccentricity (Glauber MC)
 - ✧ Effect of triangular flow may be dominant for the emission region

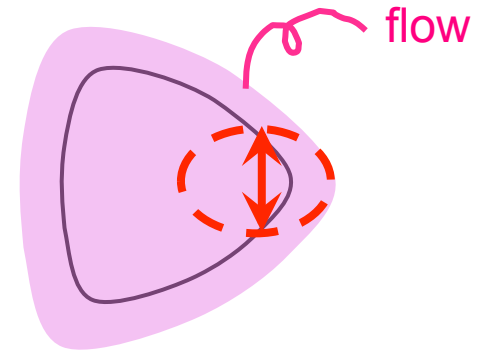
static source



w/ radial flow



w/ radial
+ triangular flow

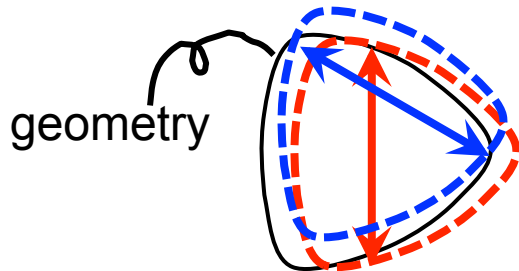


Triangular deformation can be observed via HBT?

- HBT radii w.r.t Ψ_3 don't almost show oscillation in a static source, but it appears in a expanding source. (S. Voloshin, J. Phys. G38, 124097)
- Initial triangularity is weaker than initial eccentricity (Glauber MC)
 - ✧ Effect of triangular flow may be dominant for the emission region

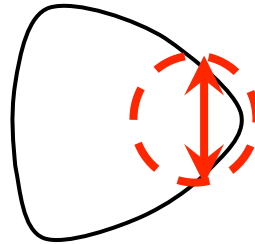
static source

 : emission region

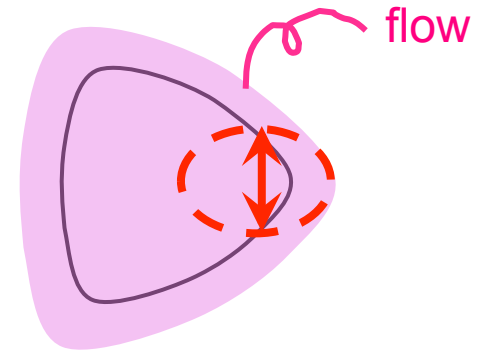


$$R_s(\Delta\varphi=0) = R_s(\Delta\varphi=\pi/3)$$

w/ radial flow



w/ radial
+ triangular flow

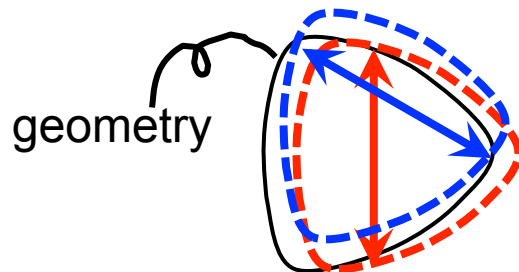


Triangular deformation can be observed via HBT?

- HBT radii w.r.t Ψ_3 don't almost show oscillation in a static source, but it appears in a expanding source. (S. Voloshin, J. Phys. G38, 124097)
- Initial triangularity is weaker than initial eccentricity (Glauber MC)
 - ✧ Effect of triangular flow may be dominant for the emission region

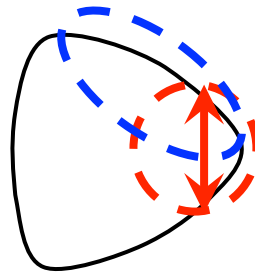
static source

 : emission region

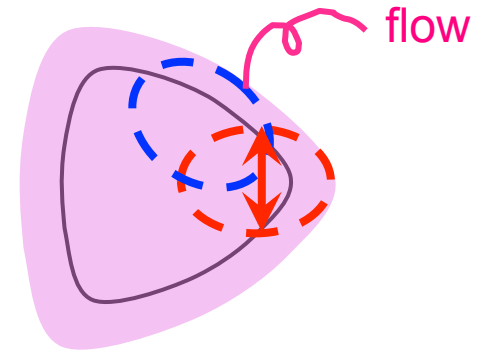


$$R_s(\Delta\phi=0) = R_s(\Delta\phi=\pi/3)$$

w/ radial flow



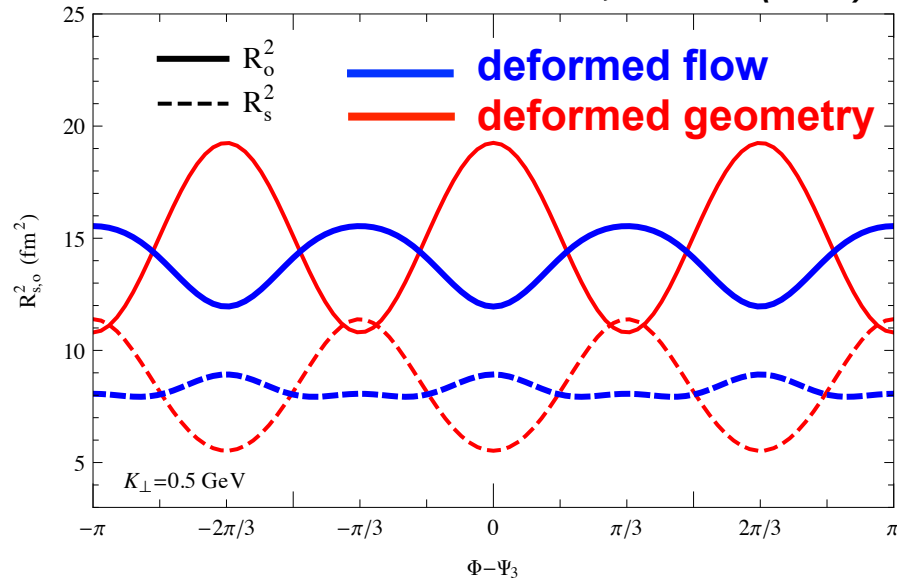
w/ radial
+ triangular flow



- HBT w.r.t Ψ_3 (also Ψ_2) results from combination of spatial and flow anisotropy
 - ✧ Need to disentangle both contributions!!

Gaussian toy model

PRC88, 044914 (2013)



■ Gaussian source including 3rd-order modulation for flow and geometry

✧ $\bar{\epsilon}_3$: triangular spatial deformation

✧ \bar{v}_3 : triangular flow deformation

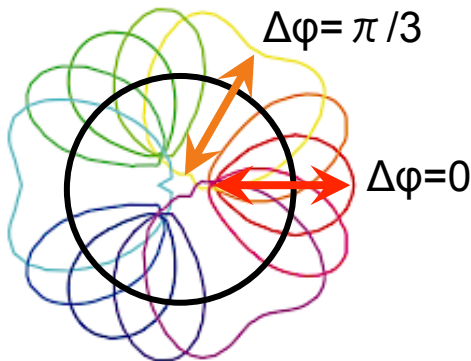
Emission function(S) and transverse flow rapidity η_t :

$$\tilde{S}(x, K) \propto \exp\left[-\frac{r^2}{2R^2} (1 + 2\bar{\epsilon}_3 \cos[3(\phi - \bar{\psi}_3)])\right]$$

$$\eta_t = \eta_f \frac{r}{R} (1 + 2\bar{v}_3 \cos[3(\phi - \bar{\psi}_3)])$$

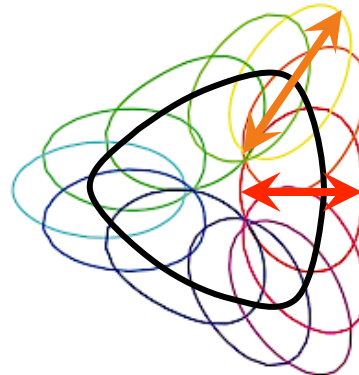
deformed flow

$$\bar{\epsilon}_3 = 0, \bar{v}_3 \neq 0$$



deformed geometry

$$\bar{\epsilon}_3 \neq 0, \bar{v}_3 = 0$$



■ Two extreme case was tested

✧ Spherical source with triangular flow(+radial flow)

✧ Triangularly deformed source with radial flow

■ “Deformed flow” shows qualitative agreement with data

Monte-Carlo simulation

■ Similar to Blast-wave model but Monte-Carlo approach

- ✧ thermal motion + transverse boost (PRC70.044907)
- ✧ introduced spatial anisotropy and triangular flow at freeze-out

■ Setup

- ✧ Woods-saxon particle distribution:

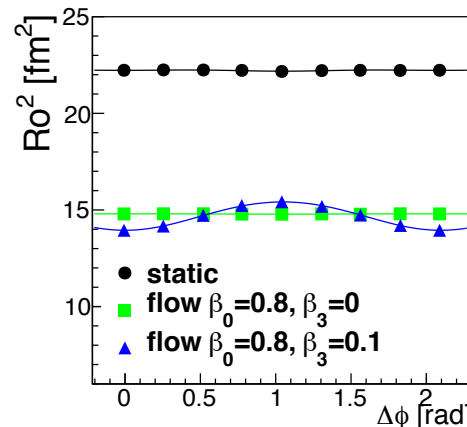
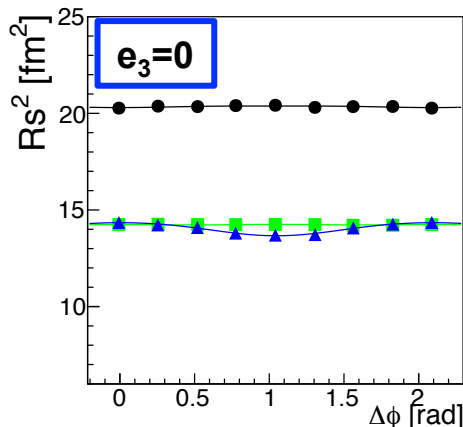
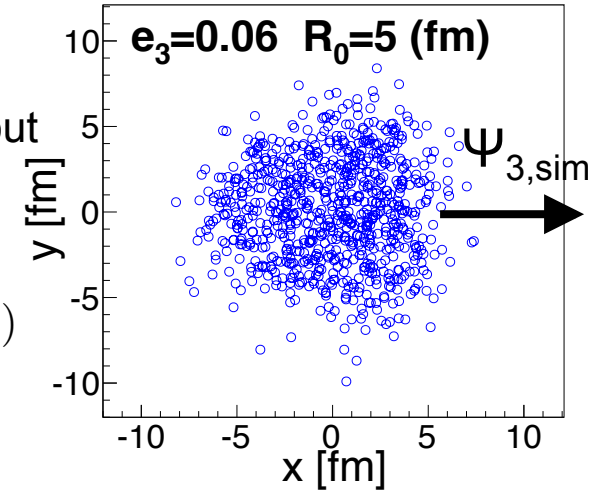
$$\Omega = 1/(1 + \exp[(r - R)/a]), \quad R = R_0(1 - 2e_3 \cos[3(\phi - \Phi)])$$

- ✧ transverse flow: $\beta_T = \beta_0(1 + 2\beta_3 \cos[3(\phi - \Psi)])$

- ✧ HBT correlation: $1 + \cos(\Delta x \cdot \Delta p)$

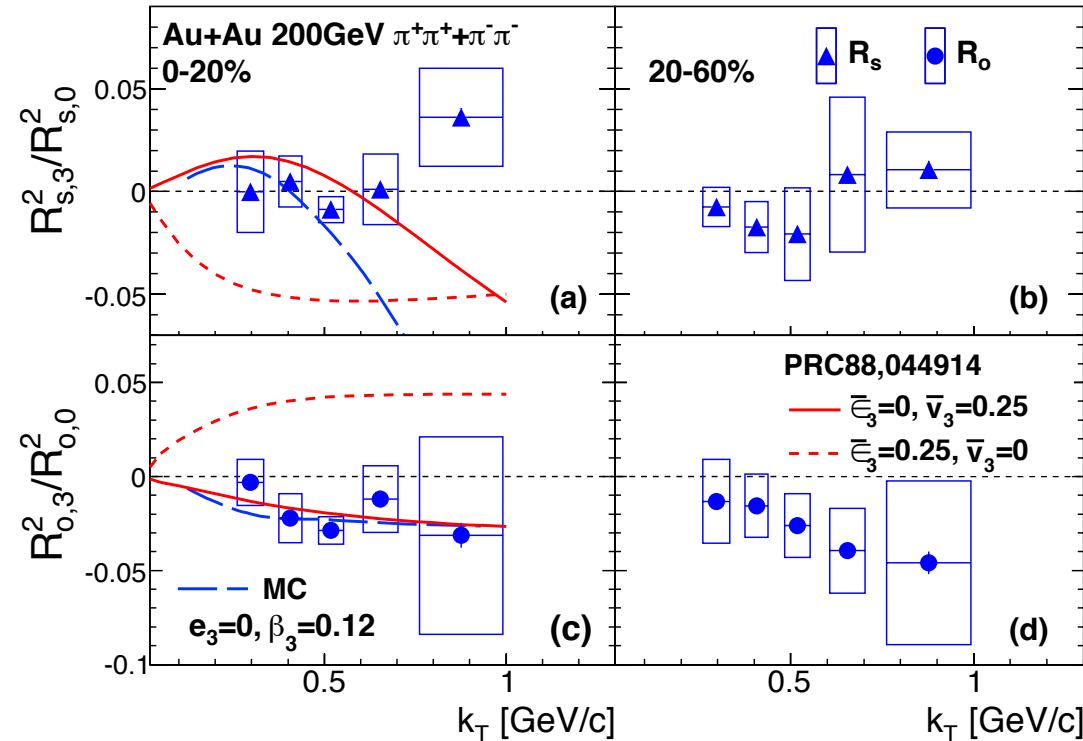
- ✧ parameters like T_f (temperature), β_0 , R_0 were tuned by spectra and mean HBT radii

✧ Assuming the spatial and momentum dist. at freeze-out



■ Oscillations of R_s^2 and R_o^2 are controlled by e_3 and β_3

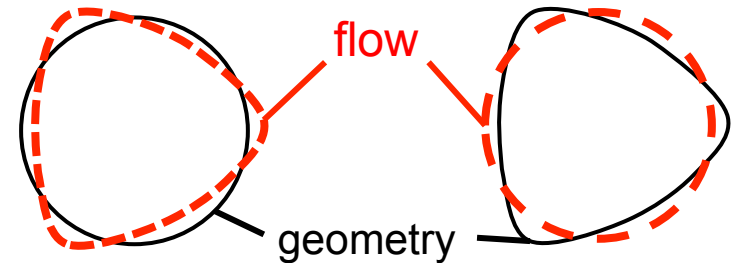
k_T dependence of 3rd-order oscillation amplitude



■ MC simulation qualitatively agrees with Gaussian toy model

deformed flow

deformed geometry



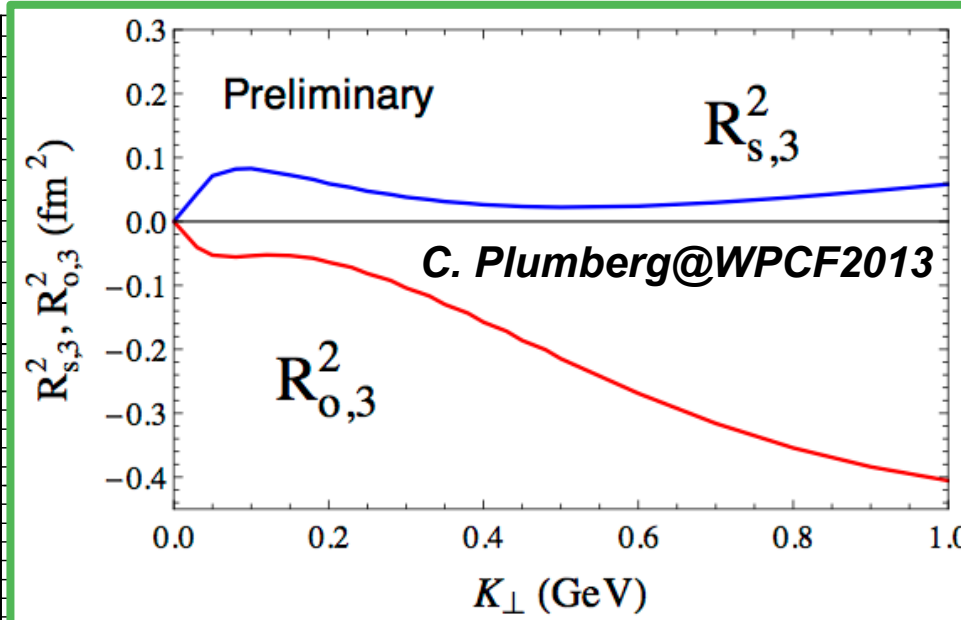
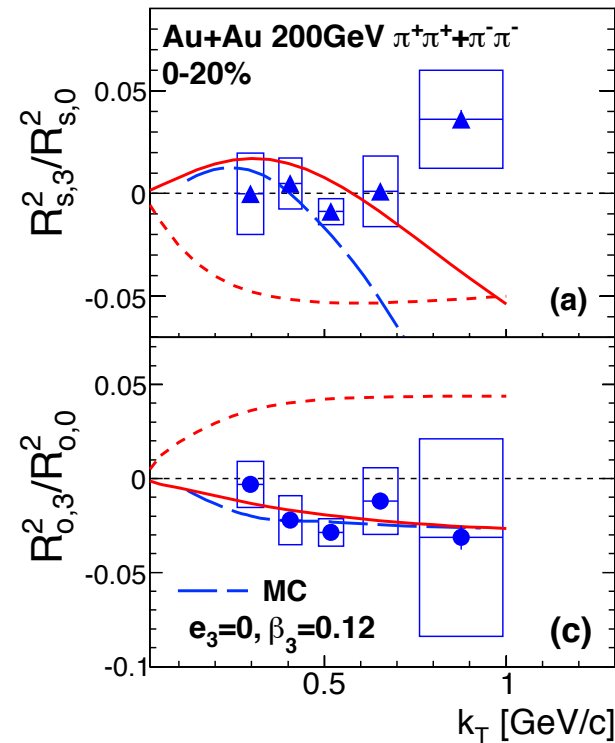
■ $R_{o,3}^2$ seems to be explained by “deformed flow” in both centralities.

✧ Note that model curves are scaled by 0.3 for the comparison with the data

■ $R_{s,3}^2$ seems to show a slight opposite trend to “deformed flow”.

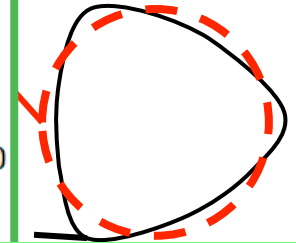
✧ Zero~negative value at low m_T , and goes up to positive value at higher m_T

k_T dependence of 3rd-order oscillation amplitude



Qualitatively
Gaussian toy model

deformed geometry

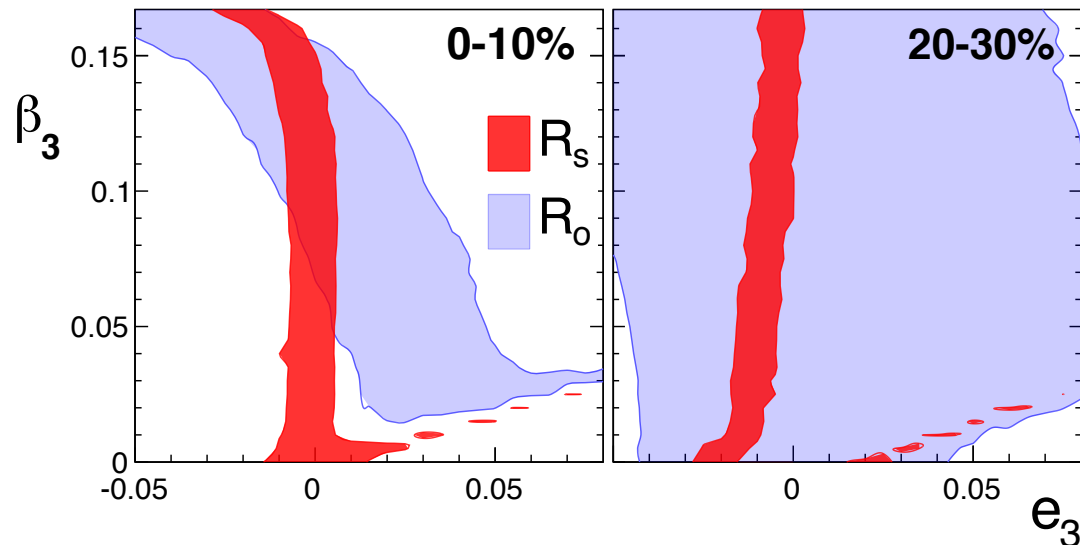


Behavior of $R_{s,3}^2$ at higher k_T may be reproduced by a full hydrodynamic calculation.

- $R_{o,3}^2$ seems to be explained by “deformed flow” in both centralities.
 - ✧ Note that model curves are scaled by 0.3 for the comparison with the data
- $R_{s,3}^2$ seems to show a slight opposite trend to “deformed flow”.
 - ✧ Zero~negative value at low k_T , and goes up to positive value at higher k_T

Constrain spatial(e_3) and flow(β_3) anisotropy

- MC simulation are compared to data varying e_3 and β_3
- χ^2 minimization: $\chi^2 = (([R_{\mu,3}^2/R_{\mu,0}^2]^{\text{exp}} - [R_{\mu,3}^2/R_{\mu,0}^2]^{\text{sim}})/E)^2$
where E is experimental uncert.. Shaded areas show $\chi^2 < 1$.

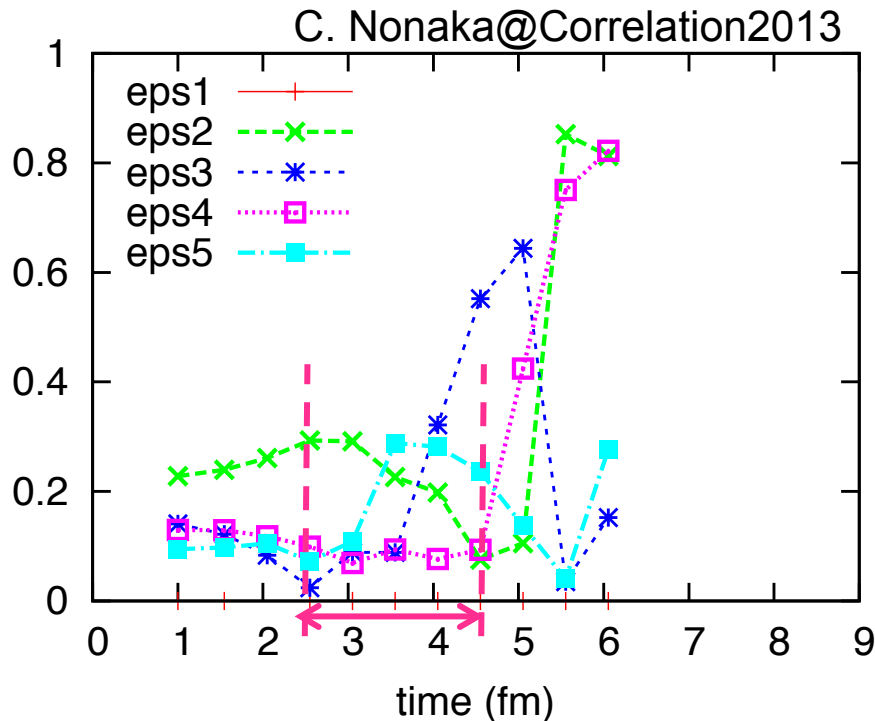


- e_3 is well constrained by R_s , less sensitivity to β_3
- Overlap of R_s and R_o shows positive β_3 and zero e_3 in 0-10%
- R_s seems to favor negative e_3 in 20-30%
- Triangular deformation is reversed at freeze-out?

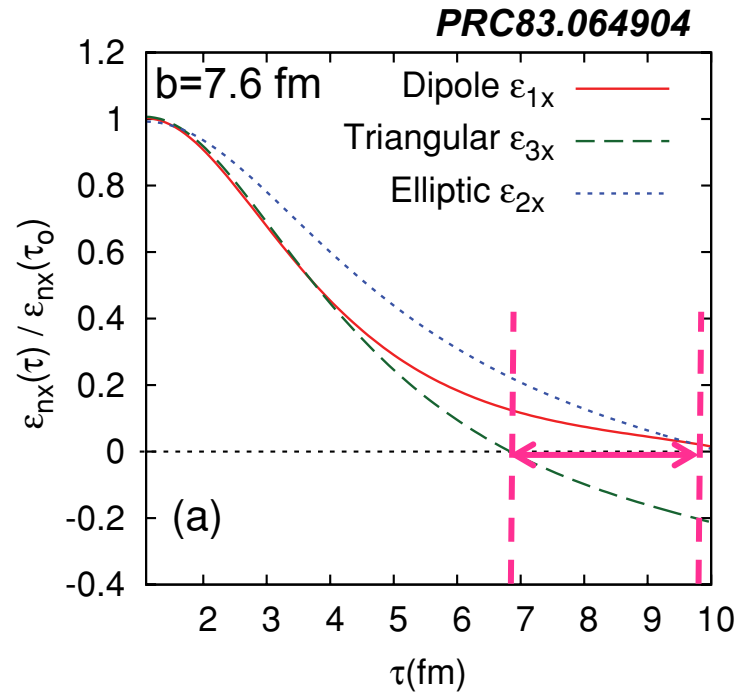
Time evolution of spatial anisotropy

■ MC-KLN + e-b-e Hydrodynamics

✧ 15-20%, Parameters are not tuned.



■ IC with cumulant expansion + ideal Hydrodynamics



- The time that ϵ_3 turns over is faster than ϵ_2 in the hydrodynamic models.
- Comparison with (e-b-e) full hydrodynamics may constrain the space-time picture of the system.

Summary

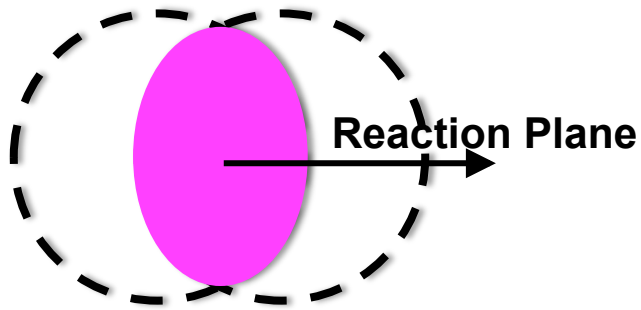
- **Azimuthal angle dependence of HBT radii w.r.t 2nd- and 3rd-order event planes was measured at PHENIX**
 - ✧ Finite oscillation of R_o^2 is seen for 3rd-order event plane as well as 2nd-order.
 - ✧ Gaussian toy model and MC simulation were compared with data. They suggest that R_o oscillation comes from triangular flow.
 - ✧ χ^2 minimization by MC simulation shows finite β_3 and zero \sim slightly negative e_3 , which may imply that initial triangular shape is significantly diluted, and possibly reversed by the medium expansion

THANK YOU!

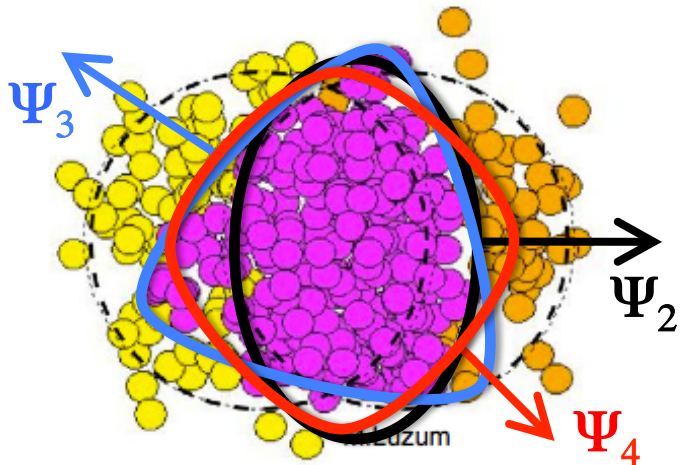
Higher Harmonic Flow and Event Plane

- Initial density fluctuations cause higher harmonic flow v_n
- Azimuthal distribution of emitted particles:

smooth picture



fluctuating picture



$$\frac{dN}{d\phi} \propto 1 + 2v_2 \cos 2(\phi - \Psi_2) + 2v_3 \cos 3(\phi - \Psi_3) + 2v_4 \cos 4(\phi - \Psi_4)$$

$$v_n = \langle \cos n(\phi - \Psi_n) \rangle$$

v_n : strength of higher harmonic flow

Ψ_n : higher harmonic event plane

ϕ : azimuthal angle of emitted particles

Correlation Function

■ Experimental Correlation Function C_2 is defined as:

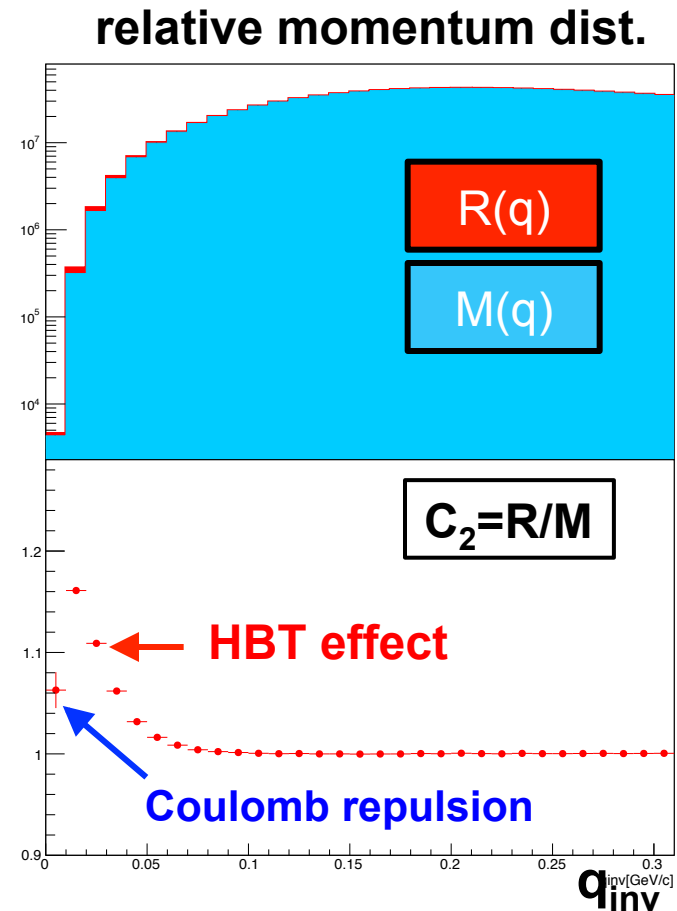
- ✧ $R(q)$: **R**ead pairs at the same event.
- ✧ $M(q)$: **M**ixed pairs selected from different events.

Event mixing was performed using events with similar z-vertex, centrality, E.P.

$$C_2 = \frac{R(q)}{M(q)}$$

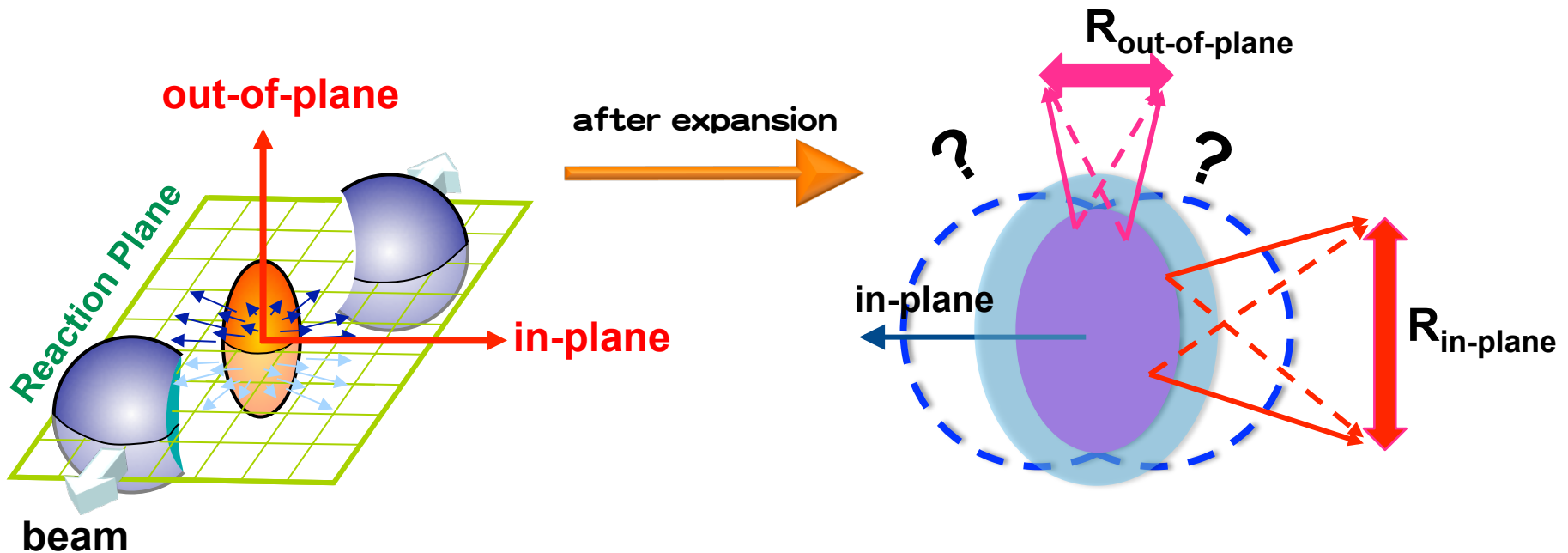
$$q = p_1 - p_2$$

- ✧ Real pairs include HBT effects, Coulomb interaction and detector inefficient effect. Mixed pairs doesn't include HBT and Coulomb effects.



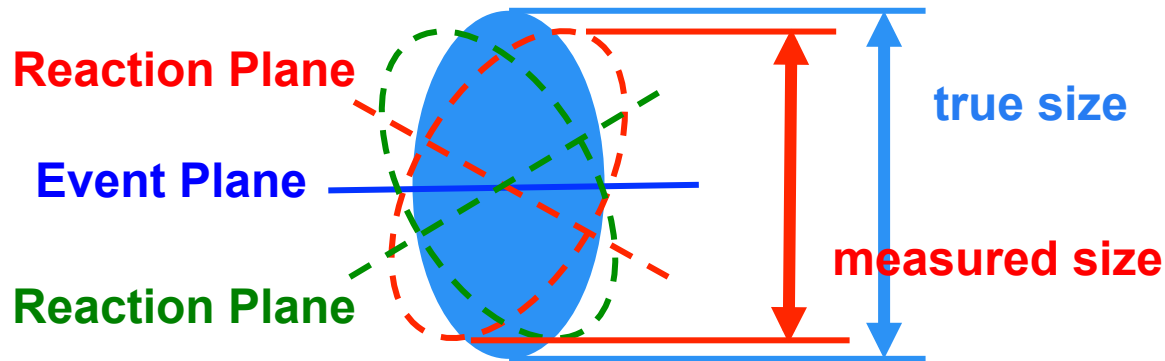
Spatial anisotropy at final state

- Angle dependence of HBT radii relative to Reaction Plane reflects the source shape at kinetic freeze-out.
- Initial spatial anisotropy causes momentum anisotropy (flow anisotropy)
 - ✧ One may expect in-plane extended source at freeze-out
- Final source eccentricity will depend on initial eccentricity, flow profile, expansion time, and viscosity etc.



Correction of Event Plane Resolution

■ Smearing effect by finite resolution of the event plane



■ Correction for q-distribution $A_{corr}(q, \Phi_j) = A_{uncorr}(q, \Phi_j)$

✧ PRC.66, 044903(2002)

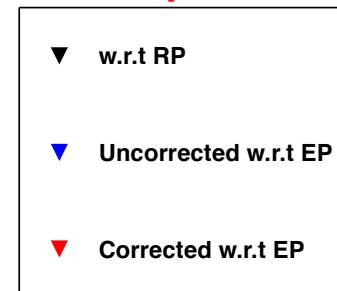
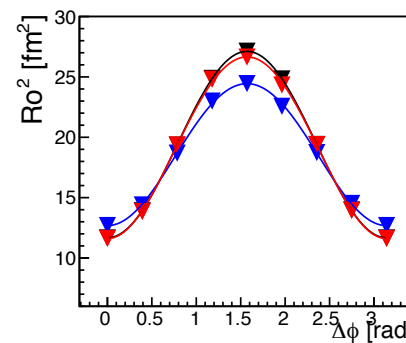
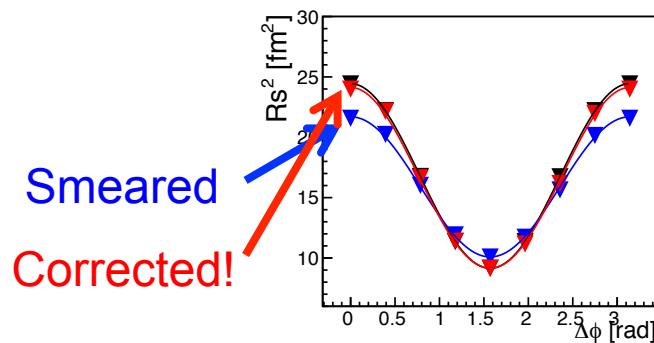
✓ model-independent correction

✧ Checked by MC-simulation

$$+ 2 \sum \zeta_{n,m} [A_c \cos(n\Phi_j) + A_s \sin(n\Phi_j)]$$

$$\zeta_{n,m} = \frac{n\Delta/2}{\sin(n\Delta/2) \langle \cos(n(\Psi_m - \Psi_{real})) \rangle}$$

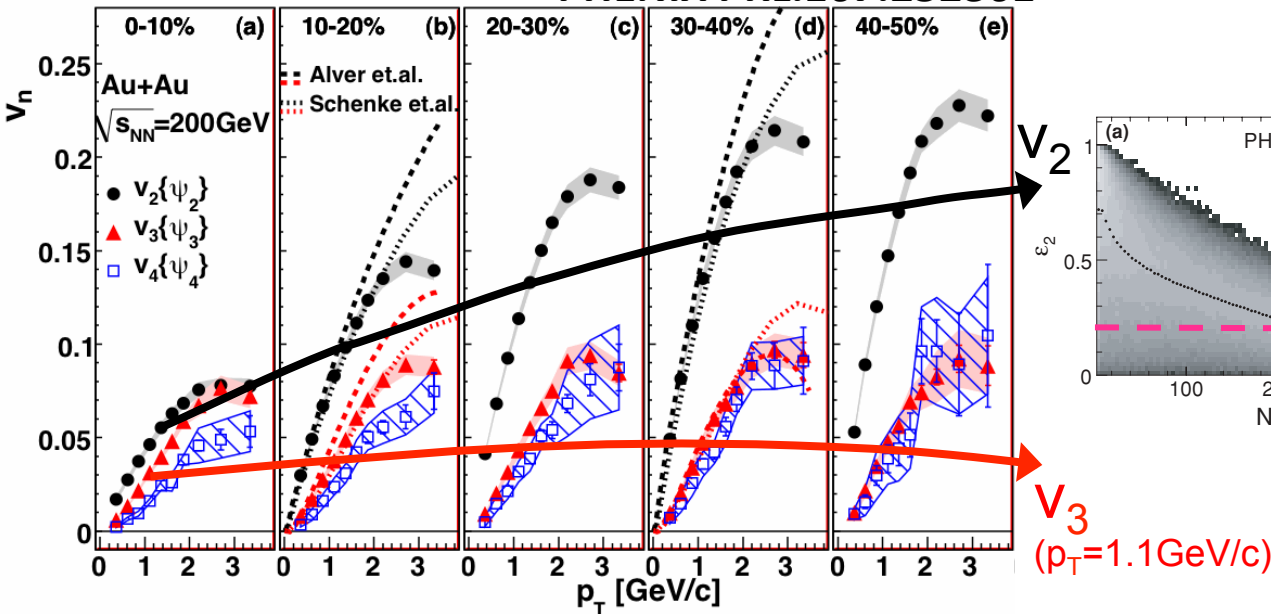
event plane resolution



Centrality dependence of v_n and initial ϵ_n

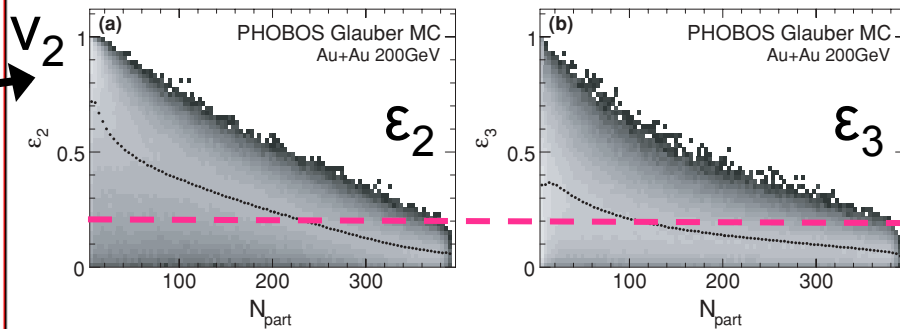
Higher harmonic flow v_n

PHENIX PRL.107.252301



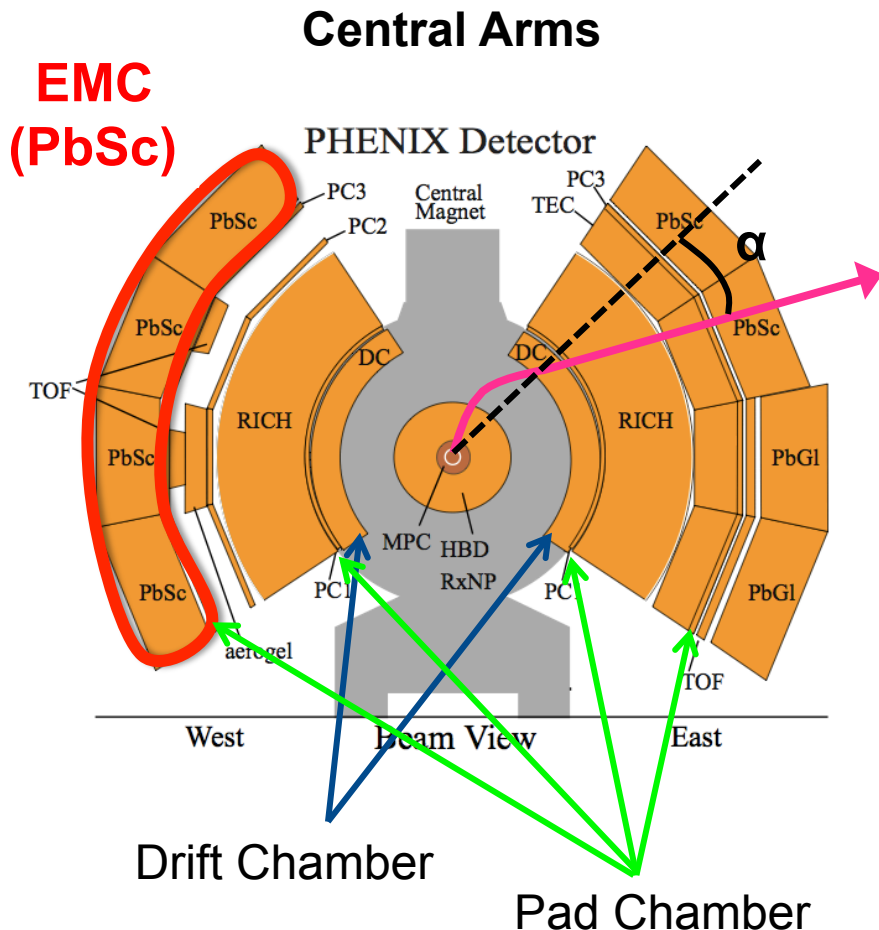
Initial source anisotropy ϵ_n

PRC.81.054905



- Weak centrality dependence of v_3 unlike v_2
- Initial ϵ_3 has finite values and weaker centrality dependence than ϵ_2 in Glauber MC simulation
- 🔵 **Triangular component in source shape exists at final state?**
➡ Measurement of HBT radii relative to Ψ_3

Track Reconstruction



■ Drift Chamber

- ✧ Momentum determination

$$p_T \simeq \frac{K}{\alpha} \quad \begin{array}{l} K: \text{field integral} \\ \alpha: \text{incident angle} \end{array}$$

■ Pad Chamber (PC1)

- ✧ Associate DC tracks with hit positions on PC1
 - ✓ p_z is determined

■ Outer detectors (PC3, TOF, EMCal)

- ✧ Extend the tracks to outer detectors